Water Research 218 (2022) 118485

Contents lists available at ScienceDirect

Water Research

journal homepage: www.elsevier.com/locate/watres

Aquifer heterogeneity controls to quality monitoring network performance for the protection of groundwater production wells

Theo S. Sarris *, Allanah Kenny, David M. Scott, Murray E. Close

Institute of Environmental Science and Research (ESR), Christchurch, New Zealand

ARTICLE INFO

Keywords:
Heterogeneity
Risk corrected detection rate
Contaminant transport
Dispersion
Monitoring network
Groundwater contamination

ABSTRACT

A groundwater monitoring network surrounding a pumping well (such as a public water supply) allows for early contaminant detection and mitigation where possible contaminant source locations are often unknown. This numerical study investigates how the contaminant detection probability of a hypothetical sentinel-well monitoring network consisting of one to four monitoring wells is affected by aquifer spatial heterogeneity and dispersion characteristics, where the contaminant source location is randomized. This is achieved through a stochastic framework using a Monte Carlo approach. A single production well is considered that results in converging non-uniform flow close to the well. Optimal network arrangements are obtained by maximizing a weighted risk function that considers true and false positive detection rates, sampling frequency, early detection, and contaminant travel time uncertainty. Aquifer dispersivity is found to be the dominant parameter for the quantification of network performance. For the range of parameters considered, a single monitoring well screening the full aquifer thickness is expected to correctly and timely identify at least 12% of all incidents resulting in contaminants reaching the production well. This proportion increases to a global maximum of 96% for a network consisting of four wells and very dispersive transport conditions. Irrespective of network size and sampling frequency, more dispersive transport conditions result in higher detection rates. Increasing aquifer heterogeneity and decreasing aquifer spatial continuity also lead to higher detection rates, though these effects are diminished for networks of 3 or more wells. Statistical anisotropy has no effect on the network performance. Earlier detection, which is critical for remedial action and supply safety, comes with a significant cost in terms of detection rate, and should be carefully considered when a monitoring network is being designed.

Introduction

Public water supply wells are monitored at regular intervals for various water quality indicators to detect pathogen, nutrient and chemical contamination that can occur from agricultural and urban activities. However, despite these measures, waterborne outbreaks are regularly reported in North America, Europe and elsewhere (Moreira and Bondelind 2016; Onyango et al. 2015), indicating that testing the production well alone does not provide sufficient warning for mitigation actions to be successful. Furthermore, in areas of significant seismic activity and following large earthquake events, groundwater is prone to pollution from damaged wastewater infrastructure (Ishii et al. 2021; Kang et al. 2013; Kobayashi et al. 2021; Sarikaya and Koyuncu 1999) and changes to the permeability of aquifer and aquitards (Elkhoury et al. 2006; Zhang et al. 2019; Liu et al. 2010), that may affect groundwater quality and safety (Nakagawa et al. 2021; Wang et al. 2016; Wang et al. 2004).

A common protective measure is to restrict the land use surrounding supply wells (USEPA 1987), however complete restriction is often impractical or impossible (particularly in urban areas), and the full extent of the well capture zone is almost always uncertain (Frind and Molson 2018). The use of a monitoring network surrounding a supply well allows for early detection and remediation (Nowak et al. 2015) that, depending on the contaminant, can include various treatment techniques such as adsorption (Fang et al. 2022), permeable reactive barriers (Burbery et al. 2020; Bortone et al. 2019) and biological techniques (Da'ana et al. 2021; Gibert et al. 2022). However, the network success rate depends on several factors such as the number and location of the sentinel wells and the sampling frequency (Bode et al. 2016; Bolster et al. 2009; Papapetridis and Paleologos 2012; Bode et al. 2018).

The design of a monitoring system typically aims to maximize contamination detection rates to minimize establishment and

* Corresponding author.
E-mail address: theo.sarris@esr.cri.nz (T.S. Sarris).

https://doi.org/10.1016/j.watres.2022.118485
Received 26 January 2022; Received in revised form 4 April 2022; Accepted 19 April 2022
Available online 21 April 2022

maintenance costs (i.e. minimize the number of sentinel wells and sampling frequency required), and to detect contamination as early as possible so that mitigation options can be implemented before contaminants reach the production well (Nowak et al. 2015; Bode et al. 2016). For landfill monitoring applications the design objectives often take the form of minimizing the plume remediation cost (Storck et al. 1997; Hudak 2001, 2002, 2005; Bierkens 2006; Salamon et al. 2006; Mahjouri and Shamsoddinpour 2016). Additional uncertainty arises when the location of the contaminant source is unknown, and the transport velocities vary greatly due to aquifer heterogeneity. The conflicting objectives result in a multi-objective optimization problem that needs to account for these uncertainties.

Several site-specific studies have addressed the optimization problem using a number of different formulations of the objective function (see discussion in Bode et al. 2016, and Sreekanth et al. 2017), while Winter and Tartakovsky (2008) and Bolster et al. (2009) propose a probabilistic risk assessment framework that represents the progress of contamination as a Markovian sequence based on a rare event statistical approximation. The common ground of these studies is that the source location is either known or randomly occurring within high-risk regions, such as within a landfill. There is little discussion in the literature on the effect of uncertainty on the optimal network design. Randomly occurring instantaneous source locations have been investigated numerically by Yenigül et al. (2005) who concluded that transverse dispersivities have significant influence on the reliability of monitoring arrays, while Papapetridis and Paleologos (2011) evaluated the effect of sampling frequency and heterogeneity level on the contaminant detection probability from a landfill, using sentinel well arrays with predetermined geometries, and concluded that detection probability decreases with increased heterogeneity. They proposed a risk function that accounts for action lag (time between detection and mitigation implementation) and investigated how increased lag can affect the system performance. Yenigül et al. (2013) considered a random permanent contaminant source originating from a landfill and concluded that a large number of monitoring wells near the potential source would be preferable, but when installation and operating costs are high, optimal solutions lead to smaller numbers of wells at greater distances from the source. Bode et al. (2016) considered quality monitoring networks in heterogeneous well capture zones, and they attempted to simplify the problem of random contamination sources with the introduction of a line of attack near the production well. This simplification led to the suggestion that very high numbers of monitoring wells may be required, while no consideration had been given to how the number of wells and contaminant detection rates may be affected by aquifer heterogeneity.

More recently, de Barros et al. (2016) analyzed the attenuation characteristics of a non-conservative contaminant in heterogeneous formations and concluded that the probability of exceeding an accepted hazard index threshold in a pumping well decreases with increased heterogeneity. The authors attributed their findings to the presence of low conductivity zones that can significantly increase the travel time between the source and the sink.

Despite considerable progress, there exist significant gaps in our fundamental understanding of how aquifer heterogeneity can affect the probabilistic description of plume migration and contaminant detection (Gómez-Hernández et al. 2017). This study addresses some of these issues by investigating the case of a permanent, conservative contaminant leakage from a random source into a heterogenous aquifer stressed by a single supply well with a fixed pumping rate, resulting in a non-uniform flow field converging towards the well. This work was prompted by earthquake related damage to underground infrastructure upgradient of a well field and under such conditions the approximate location of a contaminant source is not always known. We investigate how the contaminant detection probability is affected by aquifer spatial heterogeneity and dispersion characteristics by considering a hypothetical monitoring network of varied number of wells and sampling frequency. In this study the monitoring network follows the concept of "line of defense" presented by Bode et al. (2018), and is designed to detect contamination from unknown sources without source risk prioritizations and to provide sufficient warning for mitigation measures to be implemented to ensure the safety of the water supply. This is achieved through a stochastic framework using a Monte Carlo approach.

Model description

Our study involves the simulation of flow and contaminant transport in an unconfined, heterogeneous, alluvial aquifer. The model used in this study is based on a simplified version of HAM3 (Gyopari 2014), a 3D regional flow model of the Waiwhetu Aquifer in New Zealand's North Island. HAM3 has been rigorously calibrated and verified and has been used over the last 8 years for the sustainable management of the Waterloo borefield. Water taken from the borefield complements Wellington's drinking water supply.

The model domain is 3 km long in the mean direction of flow, 2 km wide, and is discretized by a uniform 5 m x 5 m finite difference grid (Fig. 1). Steady state flow is imposed by constant head boundaries (resulting in head gradient i = 4.67E-4 m/m) and uniform recharge across the model domain (r = 6.1E-4 m/d) (Gyopari 2014). A fully penetrating well extracts water ($Q = -10{,}000$ m^3/d) for a public supply network and is located 2 km downgradient in the flow direction. The model horizontal dimensions are considered much larger than the average aquifer thickness, and flow and transport conditions are assumed to be vertically uniform in the fully penetrating pumping and monitoring wells (Papapetridis and Paleologos 2011; Meyer et al. 1994).

The aquifer heterogeneity is addressed through the hydraulic conductivity. Hydraulic conductivity distributions in alluvial aquifers are often assigned according to hydrofacies attributed to the depositional environment (Zhu et al. 2017) and represented by multi-indicator methods (de Barros et al. 2016; Fiori et al. 2013). Here, due to the small scale and low connectivity of the most permeable hydrofacies (Burbery et al. 2018), hydraulic conductivity ($K(\mathbf{x})$) is assumed to be a lognormally distributed (such that $Y(\mathbf{x}) = \ln K(\mathbf{x})$ is a normal variate), stationary, second order and anisotropic process (Gelhar 1986; Paleologos et al. 2000; Paleologos and Sarris 2011), which has been shown to be a reasonable representation of aquifer heterogeneity for the prediction of observed plume propagation in similar environments (Sarris et al. 2018). The degree of aquifer heterogeneity is associated with the variance of $Y(\mathbf{x})$, σ_Y^2. The spatial continuity of the log transformed $K(\mathbf{x})$ field is described by an anisotropic exponential covariance model C_Y, of integral scale λ, given by:

$$C_Y(\boldsymbol{r}) = \sigma_Y^2 exp\left[-\left(\sum_{i=1}^{2}\frac{r_i^2}{\lambda_i^2}\right)\right]^{1/2} \quad (1)$$

where r_i is the separation distance between two arbitrary locations in the i^{th} direction, while the correlation length λ_i is the length over which covariance decreases by a factor of e^{-1} in direction i (Deutsch and Journel 1997). The exponential variogram correlation length in the mean flow direction (λ), statistical anisotropy ($I=\lambda/\lambda_T$) (where T denotes the transverse direction), and the log-K variance (σ_Y^2) are used to parameterize the aquifer heterogeneity, while the log-K mean (μ_Y) and effective porosity (n_{eff}) are considered as deterministic parameters and are adopted from Gyopari (2014), with μ_Y = 6.86 and n_{eff} = 0.25. Table 1 summarizes the deterministic parameters used in the flow and transport modeling.

To our knowledge, there have been no previous studies addressing solute or pathogen transport in the study area. As groundwater velocities in the study area are high, molecular diffusion becomes negligible compared to mechanical dispersion and the dispersion mechanism can be represented by the mechanical dispersion alone (Zheng and Wang 1999). Contaminant dispersion is parameterized using the longitudinal dispersivity (α) and transverse dispersivity ratio (α_T/α) based on numerical and experimental results from similar environments in New

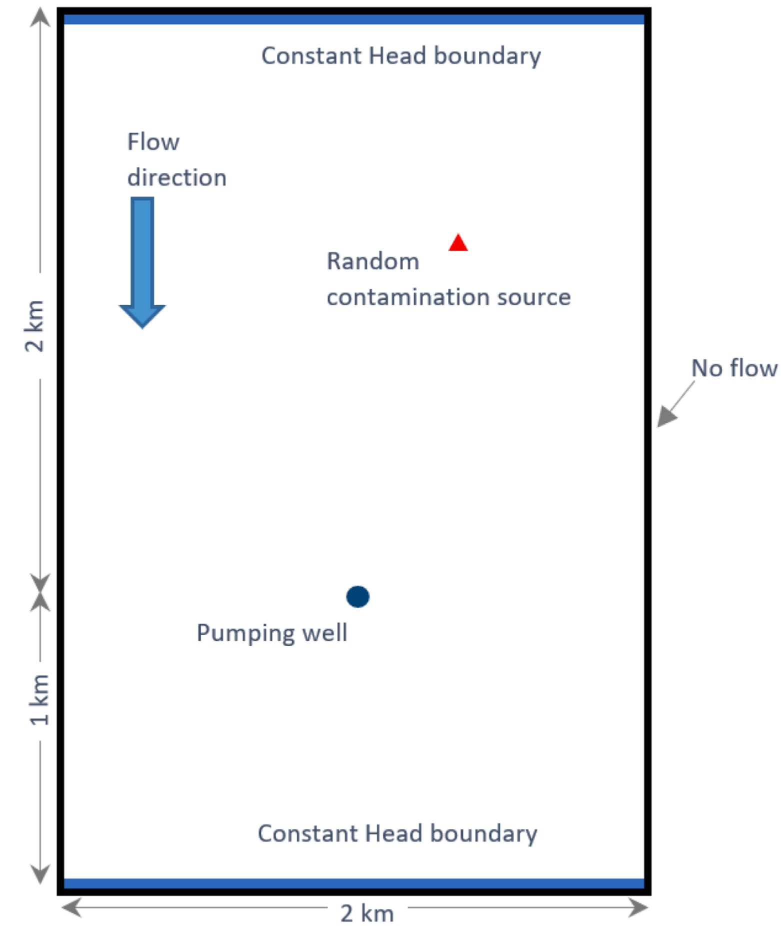

Fig. 1. Schematic diagram of the 3 km x 2 km model domain.

Table 1
Deterministic hydraulic and geological parameters of the investigation area.

Parameter	Value
Groundwater recharge	0.00061 m/d
Regional hydraulic gradient	0.000467 m/m
Pumping rate	10,000 m^3/d
Hydraulic Conductivity ln-mean	6.86
Porosity	0.25

Zealand (Sarris et al. 2018) and previously published results (Zech et al. 2015).

A source at a random location is assumed to release a conservative, fully soluble contaminant in the aquifer. In the study area there has been evidence of solute and pathogen contamination recently following the 2016 Kaikoura earthquake (7.8 M_W), but to the authors' knowledge there have been no studies quantifying these accidental discharges. Contaminants are assumed to be released at a constant rate resulting in an average source strength (C_0). In most cases contaminants are expected to undergo some form of geochemical or biological transformation, resulting in mass and concentration reductions (Renou et al. 2008). These reductions are heavily dependent on the contaminant, but also on the aquifer's physical, chemical, and biological environment. Such processes are not considered here, as the focus of our study is the impact of aquifer heterogeneity, monitoring locations, and sampling frequency on contaminant detection probabilities. The source is assumed steady state (Yenigül et al. 2013), which physically corresponds to a source that remains active (and potentially undetected or not remedied) for sufficient time for the plume to potentially reach the pumping well. Under these conditions the transport of contaminants in Fickian groundwater flow systems can be expressed as (Zheng and Wang 1999; Sarris et al. 2018):

$$\frac{\partial(\theta C)}{\partial t} = \nabla\cdot(\theta D\cdot\nabla C) - \nabla\cdot(\theta v_i C) + q_s C_s \tag{2}$$

where D is the mechanical dispersion coefficient tensor, v_i is the linear pore water velocity defined as q_i/θ and relates the transport to the flow equation, and C_s is the concentration of the source fluxes q_s. The components of the mechanical dispersion tensor in two dimensions are (Bear 1979; Bortone et al. 2019)

$$D_{xx} = \alpha\frac{v_x^2}{|v|} + \alpha_T\frac{v_y^2}{|v|},\ D_{yy} = \alpha\frac{v_y^2}{|v|} + \alpha_T\frac{v_x^2}{|v|},\ D_{xy} = D_{yx} = (\alpha - \alpha_T)\frac{v_x v_y}{|v|} \tag{3}$$

where $|v|$ is the magnitude of the velocity vector. Flow and transport through the unsaturated zone is not considered in our study. Cases where ignoring the influence of the vadose zone to contaminant transport is appropriate, include those where the contamination source is near or below the water table, when the water table is shallow, or when transport through the vadose zone is relatively fast through non-stratified media and/or fingered flow conditions (Wang et al. 2018; Sarris, Scott, et al. 2019).

Monte Carlo scheme

The flow and transport in the heterogeneous aquifer are studied in a stochastic framework, using a Monte Carlo approach, as follows:

For each combination of a set of flow (λ, I and σ_Y^2) and transport (α, α_T/α) model parameters, two dimensional random hydraulic conductivity fields are generated using the Sequential Gaussian Simulation method (Deutsch and Journel 1997). Aquifer heterogeneity and dispersion parameter values considered in this study have been selected to represent a range of heterogeneous environments (Gelhar 1986; Sarris and Paleologos 2004; Burbery et al. 2020; Fiori et al. 2013; Zech et al. 2015; de Barros et al. 2016) as summarized in Table 2.

For each simulated field, a random contamination source location is selected across the study area. The numerical steady state flow solution is obtained using MODFLOW-NWT (Niswonger et al. 2011), while the transport problem is solved using MT3D-USGS (Bedekar et al. 2016). To reduce the computational burden and the prohibitive disk storage space requirements (due to the large number of realizations required for solution convergence), the transport solution is obtained for steady state transport conditions. To estimate the stochastic contaminant arrival times, advective transport travel times are obtained using MODPATH version 5 (Pollock 1994) by calculating the particle travel times from each grid cell to the sink or downgradient boundary.

Detection statistics

Once all the realizations have been undertaken, the point detection probability statistics are calculated at each grid cell. This involves the calculation of true positive (TP), true negative (TN), false positive (FP) and false negative (FN) probabilities. A positive/negative outcome refers to whether the contamination reaches the well, and true/false outcome refers to the detection of the contamination from the monitoring well. True detection is when the outcome (positive or negative) is correctly identified in terms of grid cell concentration exceeding a predefined detection limit (C_{thr})). In this study the threshold concentration at which detection occurs is $C_{thr} = 10^{-3}C_0$ (Hudak 2001). For example, the TP detection rate ($DTP_{i,j}^N$) from N total realizations at a single location (i,j) in the flow field is calculated according to:

$$DTP_{i,j}^N = \frac{1}{N_{pos}} \sum_{n=1}^{N} TP_{i,j}^n \quad (4)$$

where N_{pos} is the number of positive events, and $TP_{i,j}^n$ denotes a TP detection at location (i,j) for realization *n*:

$$TP_{i,j}^n = \begin{cases} 1 \text{ if } C_w > C_{thr} \text{ and } C_{i,j} > C_{thr} \\ 0 \text{ otherwise} \end{cases} \quad (5)$$

In (5) C_w and $C_{i,j}$ are the contaminant concentrations at the pumping well and monitoring location (i,j) respectively.

For a monitoring network consisting of *k* sentinel wells, the detection rate (also known as sensitivity, or true positive rate in biostatistics) of the entire network (DTP_k) is calculated as the size of the set of realizations where at least one of *k* wells has a TP detection, divided by the total number of positive events (Yerushalmy 1947):

Table 2
Stochastic model parameter values.

Parameter	Values
λ (m): Correlation length	20, 50, 500
I (-): Statistical anisotropy ratio	1, 5, 10
σ_Y^2 (-): Log-K variance	0.1, 1.0, 2.0
α (m): Longitudinal dispersivity	0.62, 6.2, 62.0
α_T/α (-): Transverse dispersivity ratio	0.1, 1.0

$$DTP_k = \frac{1}{N_{pos}} \left| \cup_k S_{i,j}^{TP} \right| \quad (6)$$

where $S_{i,j}^{TP}$ is the set of realizations where a TP detection occurred at location (i,j):

$$S_{i,j}^{TP} = \left\{ n : TP_{i,j}^n = 1 \right\} \quad (7)$$

The term $\cup_k S_{i,j}^{TP}$ is the union of the sets for each of the *k* wells in the network, which gives the set of realizations where a TP detection occurred at any of the well locations, ignoring any duplicate cases where 2 or more wells detect the contaminant plume in the same realization. The size of this set is the total number of TP detections for the network. Therefore, a crude effectiveness measure of a *k*-well monitoring network could be obtained by calculating the network detection rate (DTP_k).

A monitoring network should, however, also provide an early indication of the imminent well contamination for remedial actions to be implemented (Bode et al. 2016), by ensuring that transport time between first arrival at the monitoring network and arrival at the pumping well will be equal to or greater than a specified threshold, T_R. For practical applications T_R is associated with the sampling frequency and action implementation timeframes. An optimal monitoring network layout can be obtained by maximizing DTP_k, such that all wells in the network satisfy the condition that the mean advective travel time T between the monitoring and pumping well is greater than T_R. A monitoring network should also minimize the risk of false positive detections, which can be significant for non-conservative and pathogenic contaminations and can result in significant supply disruptions.

Alternatively, the network effectiveness can be calculated with a risk correcting function (Papapetridis and Paleologos 2011) that considers:

a) the contamination detection rate adjusted for potential false positive detections,
b) detection timing relative to T_R, and
c) the travel time uncertainty (from the monitoring wells to the pumping well).

We propose a weighted risk function as:

$$f_{risk}^{k,\,T_R} = \frac{1}{k} \left(DTP_k - DFP_k \right) \sum_k f_{i,j}^{T_R} \times f_{i,j}^{\sigma} \quad (8)$$

where DFP_k is the false positive detection rate of a k-well network (Pagano and Gauvreau 2018) given by:

$$DFP_k = \frac{1}{N_{neg}} \left| \cup_k S_{i,j}^{FP} \right| \quad (9)$$

$S_{i,j}^{FP}$ is the set of realizations where a FP detection occurred at location (i, j) (similar to (7)), and N_{neg} is the total number of negative events. In (8) the weighting term $f_{i,j}^{T_R}$ accounts for the mean travel time T from a monitoring well located at (i,j) to the pumping well, and here is given by a sigmoid function (Ruppert et al. 2015; Sarris and Paleologos 2004) with midpoint T_R and slope $T_R/2$ that smoothly increases from 0 to 1 as T increases from 0 to $2T_R$:

$$f_{i,j}^{T_R} = \frac{1}{2} \left(1 + \tanh\left[\frac{T - T_R}{\frac{T_R}{2}} \right] \right) \quad (10)$$

This term greatly reduces the risk correcting function $f_{risk}^{k,\,T_R}$ when travel time T from a monitoring well to the pumping well is less than the threshold T_R, whereas the slope (which in (10) is set to $T_R/2$) defines the distance from T_R where f^{T_R} reaches its upper and lower limits. As a result, f^{T_R} aims to scale the effects of early and late detections, by promoting early detection beyond a simple binary threshold of the form $T > T_R$. The term $f^{\sigma}_{i,j}$ is weighting the uncertainty of the travel time estimates and here is given by:

$$f^{\sigma}_{i,j} = \frac{1}{1+\sigma^{T}_{i,j}} \tag{11}$$

where $\sigma^{T}_{i,j}$ is the average travel time standard deviation at (i,j) expressed as a percentage of the average. $f^{\sigma}_{i,j}$ is close to 1 when travel time uncertainty is low and decreases towards 0 as the uncertainty increases. It follows from (9) through (11) that $f^{k,\,T_R}_{risk}$ has a range [−1,1], but for conservative contaminants within the well capture zone where DFP reduces towards zero, its range reduces to [0,1]. As such, the quantity $f^{k,\,T_R}_{risk}$ can be considered as the risk corrected detection probability of a random contamination source by a k-well monitoring network. For the purposes of this work, risk is quantified in terms of monitoring and remedial action delays and uncertainties.

Results and discussion

Number of realizations

The number of realizations that are required for the Monte Carlo scheme solution to converge varies depending on the physical problem and the sources of uncertainty. In our study the scheme is considered to have converged when the TP and TN detection rates stabilize after a sufficient number of realizations (Lahkim and Garcia 1999; Yenigül et al. 2005). The term $\Delta DTP^{n}_{i,j}$ is defined as the change of the TP rates across the numerical grid (denoted by the indices i and j) after n realizations according to:

$$\Delta DTP^{n}_{i,j} = DTP^{n}_{i,j} - \frac{1}{n-1}\sum_{k=1}^{n-1} DTP^{k}_{i,j} \tag{12}$$

The $\Delta DTP^{n}_{i,j}$ standard deviation σ^{n}_{TP} for the n^{th} realization can be calculated across the numerical grid. In a similar manner $\Delta DTN^{n}_{i,j}$ and σ^{n}_{TN} can be calculated for the TN detection rates. In our study the sum of σ^{n}_{TP} and σ^{n}_{TN} is used as the convergence criterion. Fig. 2a plots the scheme convergence with increasing number of Monte Carlo realizations for low dispersivity and heterogeneity, whereas Fig. 2b plots the scheme convergence for the case with high dispersivity and high heterogeneity. These figures indicate that the number of realizations to achieve convergence increases with increased heterogeneity and more dispersive conditions (Paleologos et al. 2000), but convergence can be attained with 10,000 to 15,000 realizations for all cases. The latter number is chosen for our numerical experiments.

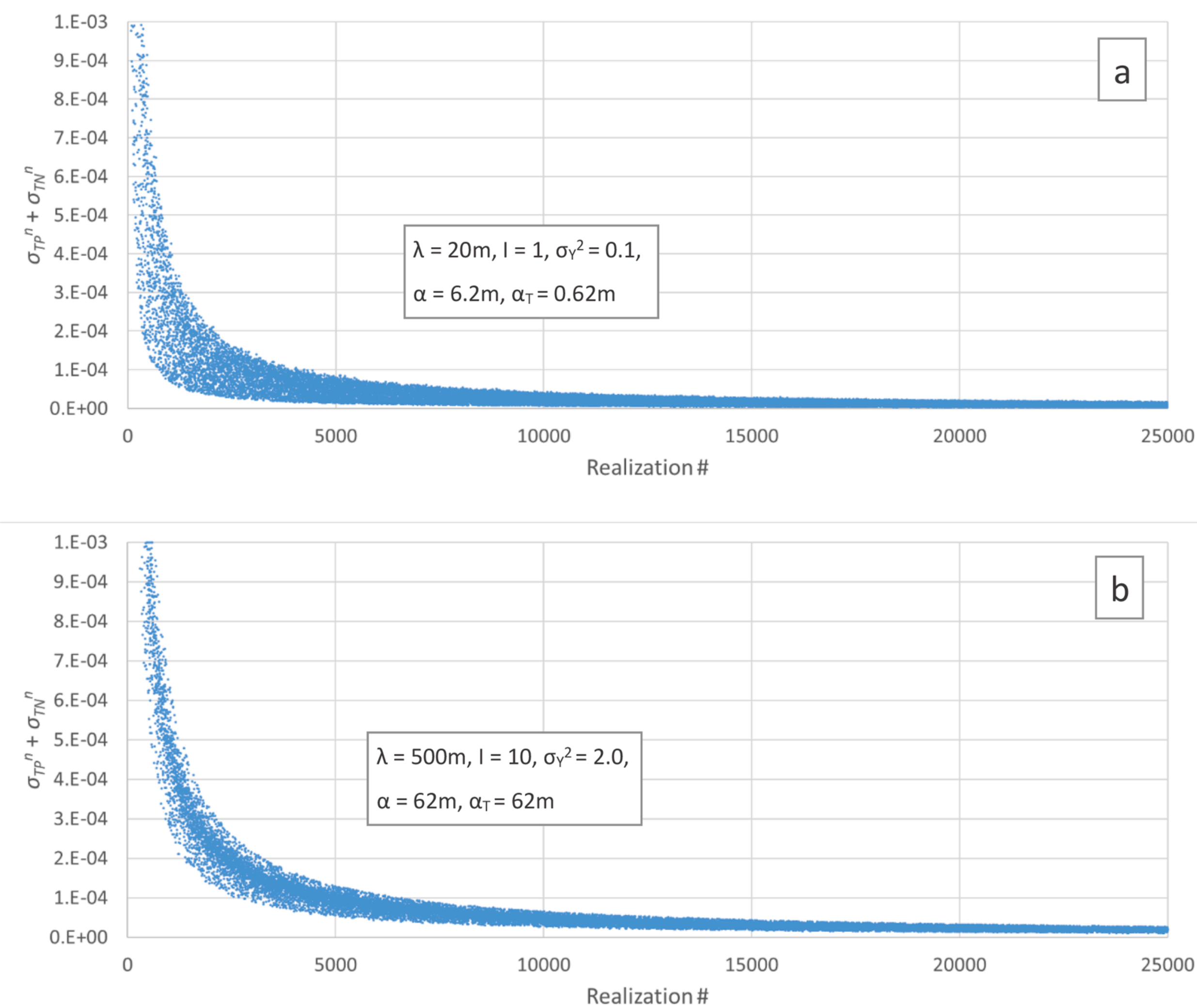

Fig. 2. Convergence of mean true positive (TP) and true negative (TN) detection probability changes for increasing number of realizations for low (a) and high (b) dispersive and heterogeneity conditions.

Contaminant travel time and detection rate

Based on the site heterogeneity conditions (Gyopari 2014; Donaldson and Campbell 1977) and similar environments in NZ (Sarris et al. 2018; Burbery et al. 2020; Sarris, Close, et al. 2019) we considered $\lambda = 50$ m, $I = 5$, $\sigma_Y^2 = 1.0$, $\alpha = 6.2$ m, $\alpha_T/\alpha = 0.1$ as base model parameters, using the ranges from Table 2 to assess their effects on contaminant detection rates. A base travel time threshold of $T_R = 100$ days is also considered, to allow time for sampling the pumping well and some response time for mitigation (Papapetridis and Paleologos 2012). This could correspond to quarterly sentinel well sampling (approx. 90 days between sampling runs) with a 10-day response time, or 60-day sampling intervals and longer response time (40 days), and so on.

The TP detection rate (Eq (4)) across the model domain for 4 different dispersivity cases is shown in Fig. 3. As expected, TP is larger around the pumping well and directly downgradient. The latter is the effect of dispersive transport at or near the well capture zone boundary. Higher TP rates indicate that a single monitoring point at this location should provide increased positive detection probabilities, when the effect of T_R is not considered, such as for the zone downgradient of the pumping well where the contamination will be detected after the plume reached the pumping well. TP increases considerably with increasing dispersivity (particularly in the transverse direction), as the lateral plume spreading facilitates detection. There is some asymmetry in TP distribution across the domain for the highly dispersive flow conditions in Fig. 3d. This is considered to be an artifact of the finite number of realizations undertaken (Lahkim and Garcia 1999; Papapetridis and Paleologos 2011; Sarris, Close, et al. 2019), however, even when the TP distribution is obtained with a total of 25,000 realizations, for the case with highest dispersivities and heterogeneity some residual (albeit smaller) asymmetry is still observed (results not shown).

Fig. 4 shows the average advective travel time from each grid cell to the pumping well and the relative travel time standard deviation, for different parameter values and increasing heterogeneity. White denotes the area where particles never reach the pumping well, while the colored area denotes the average capture zone. Note that these travel times were obtained using particle tracking considering advective transport alone, ignoring dispersive effects. When heterogeneity is low, the average travel time to the pumping well is Gaussian with little variability between realizations. With increasing heterogeneity, the capture zone size increases (Ayinippully Nalarajan et al. 2021) as does the variability between realizations, even though the range of the average travel times does not change, as shown in Figs. 4d-4f. Increasing statistical anisotropy has little effect on the spatial distribution of travel times and relative standard deviation σ^T (Figure S1). Increasing λ from 20 m to 50 m and 500 m, increases the capture zone size by 23% and 60% respectively (Figure S2), as the greater spatial continuity of the K field allows preferential transport to the pumping well from a larger part of the simulated aquifer (Cole and Silliman 1997). Increasing σ_Y^2 also contributes to increased capture zone area and is the main contributor to the significant increase of σ^T (Figure S3) (Ayinippully Nalarajan et al. 2021).

The TP and FP detection rates, average advective travel time, and resulting f_{risk} for a single monitoring location for the model base parameters are shown in Fig. 5. Unsurprisingly, FP rate peaks downgradient and to the sides of the pumping well, where monitoring is likely to detect up to 25% of contamination events that do not reach the supply well, and perhaps unnecessarily trigger remedial responses. f^{risk} in Fig. 5 has been calculated for $T_R = 100$ d In the vicinity of the pumping well f^{risk} reduces to almost zero, despite the high TP and low FP rates, as the average advective travel time T is below T_R and any monitoring outcomes would not occur until after the water supply has been contaminated. Further from this zone, f^{risk} increases sharply as T approaches T_R, before decreasing as the distance from the well increases and TP rate decreases. The area downgradient of the well with the highest f^{risk} value (shown in red in Fig. 5d) is due to both the high TP rate (Fig. 5c) and the very low σ^T (shown earlier in Fig. 4e) on the border of the capture zone. However, the calculation of the travel time, which is computed as the travel time between each grid cell and the pumping well, does not consider the contaminant source location. In most cases contaminant arrival times to the pumping well are going to be lower than to the monitoring location immediately downgradient of the well. Hence, the constraint that the travel time is greater than T_R alone, without considering simulated arrival times, is not a sufficient condition for early contamination detection in converging flows. For that reason, monitoring locations downgradient of the pumping well are not considered for monitoring network configurations.

The effect of T_R on f_{risk} for a single observation point is shown in Fig. 6. As T_R increases, the area surrounding the pumping well where $f_{risk} \simeq 0$ also increases in size. Within this zone monitoring should not be expected to have a practical benefit. The maximum f^{risk} upgradient of the well is approximately 0.32 for $T_R = 10$ d, and decreases to approximately 0.25 and 0.15 for T_R equal to 100 d and 200 d respectively. This suggests that earlier detection comes with significant reduction in the effectiveness of the monitoring scheme (Bode et al. 2016). However, this does not address the performance of monitoring networks consisting of multiple sentinel wells which is discussed in the following section.

Monitoring network optimization

A monitoring network is optimized by finding the locations that maximize the risk correcting function (Eq (8)) for a prescribed network size (i.e. number of monitoring wells). Because of the highly non-linear nature of the optimization problem and the relatively small dimensionality of the phase space (Sarris and Burbery 2018), brute force optimization is applied where the possible location combinations are sampled in sequence. As discussed earlier, possible monitoring locations are restricted to those upgradient of the pumping well. To further reduce the computational burden, the domain of possible network locations is restricted by assuming that the solution needs to be symmetric about the $X = 1$ km plane, in accordance with the average flow field symmetry.

It took approximately one hour of wall clock time to calculate an optimal 4-well network with 2 symmetric pairs of wells across a single model domain, using a single core of an Intel Xeon Gold 6150 server with 128 GB of memory and clock speed of 2.7 GHz (Sarris et al. 2021), whereas an optimal 5-well network took multiple days as the problem dimensionality greatly increases with each additional well. To reduce the computational burden, in this study network sizes ranging from 1 to 4 wells are considered.

Fig. 7 shows the effect of flow and transport parameters on the optimal array locations, while Fig. 8 summarizes the calculated detection statistics for each network. Optimal performance with a single monitoring well is always achieved with the well at the side of the capture zone and not immediately upgradient of the pumping well. Detection rates depend on the size of the monitoring network and the parameter values, and range between 12% for a single monitoring location to 96% for four monitoring wells. For landfill monitoring, under uniform flow conditions and for instantaneous sources, Papapetridis and Paleologos (2012) reported detection probabilities ranging between 5% and 35% for up to six monitoring wells, while for similar flow settings Yenigül et al. (2005) estimated detection probabilities between 5% and 80% for twelve monitoring wells, dropping to a maximum of 45% for six wells. Bode et al. (2016) reported that a network of 8 monitoring wells

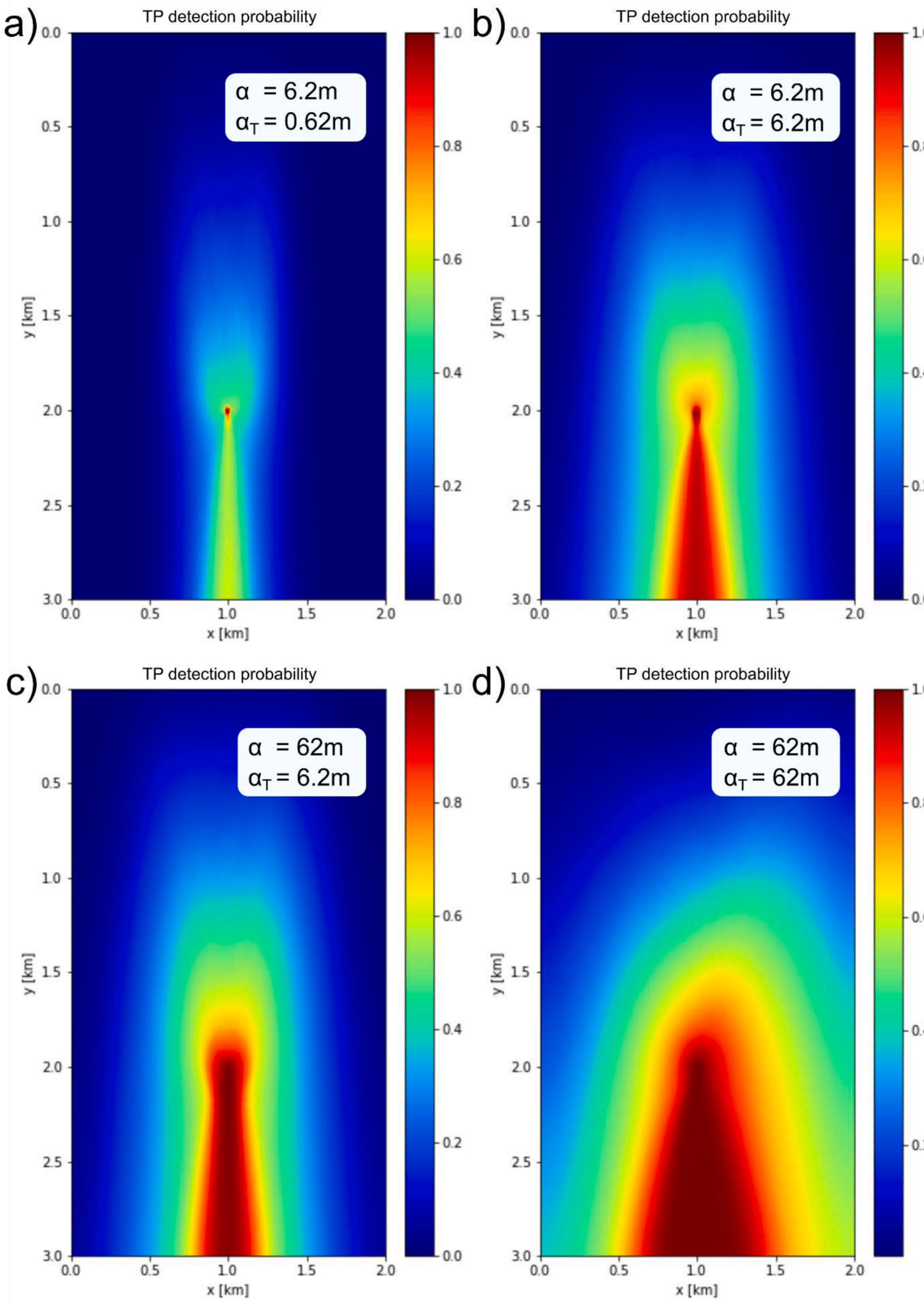

Fig. 3. True positive (TP) detection rate for varied dispersivity. The rate is highest around the pumping well and directly downgradient and increases with dispersivity (transverse dispersivity α_T in particular). Field parameters are $\lambda = 50$ m, $I = 5$ and $\sigma_Y^2 = 1.0$.

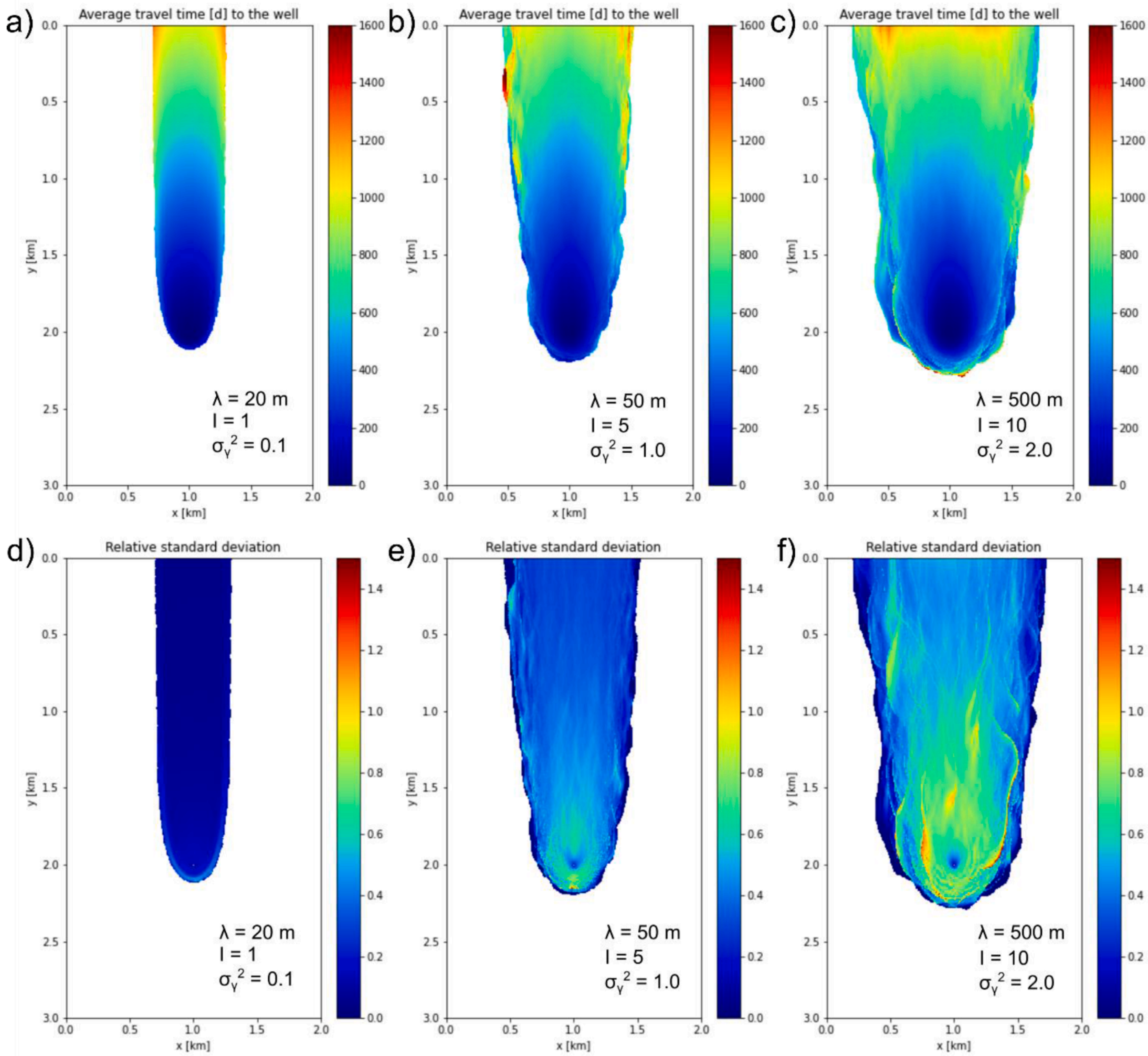

Fig. 4. a,b,c) average advective travel time to the pumping well, d,e,f) relative standard deviation in travel time for varied heterogeneity. The average travel time to the pumping well is more uniform when heterogeneity is low. The capture zone is larger when heterogeneity is high. White area. particles never reach the well. Dispersion parameters are $\alpha = 6.2$ m, $\alpha_T/\alpha = 0.1$.

placed immediately downgradient of known risk sources can provide detection probabilities of up to 91%. There are several factors contributing to the greater detection rates with smaller number of monitoring wells in this study. We only consider permanent sources in contrast to the instantaneous sources used in the aforementioned earlier studies, that make the resulting plumes harder to detect, unless a dense monitoring network is created. For landfill monitoring and for permanent sources for example, Yenigül et al. (2013) reported that detection probabilities from a 3 well network can be up to 85% if the distance from the source is large enough. To our knowledge all previous studies consider monitoring downgradient of high-risk areas under uniform flow conditions, with the exception of Bode et al. (2016), that for numerical efficiency, simulated random sources in the well capture zone with an arc of point sources that cannot account for the dispersive characteristics of plumes, which would suggest a larger number of monitoring locations is needed. In all cases of our study, DFP is small and ranges between 0% and 8%. This is to be expected since only permanent contaminant sources are considered with monitoring within the well capture zone. Instantaneous and non-conservative sources would be expected to result in greater false positive detections, with the term DFP contributing more to f_{risk}.

Our numerical results suggest that increasing longitudinal and transverse dispersivities (Figs. 7a, 8a) result in large increases in f_{risk} and TP detection rate. Under the most dispersive conditions a maximal detection rate (96%) is achieved with 4 wells, while a single well can correctly and timely identify 64% of all positive contamination events. For low α and α^T (0.62 m and 0.062 m respectively), the detection rate from a single monitoring location is only 12%, whereas a 4 well network achieves a peak detection rate of 49%. For non-convergent flow, Yenigül et al. (2005) and Papapetridis and Paleologos (2011) reported increasing detection probability with increasing transverse dispersivities, but they noted that after a threshold, and as the plume dimensions increased, concentrations reduced below the detection limit, and the detection probabilities declined. However Yenigül et al. (2013),

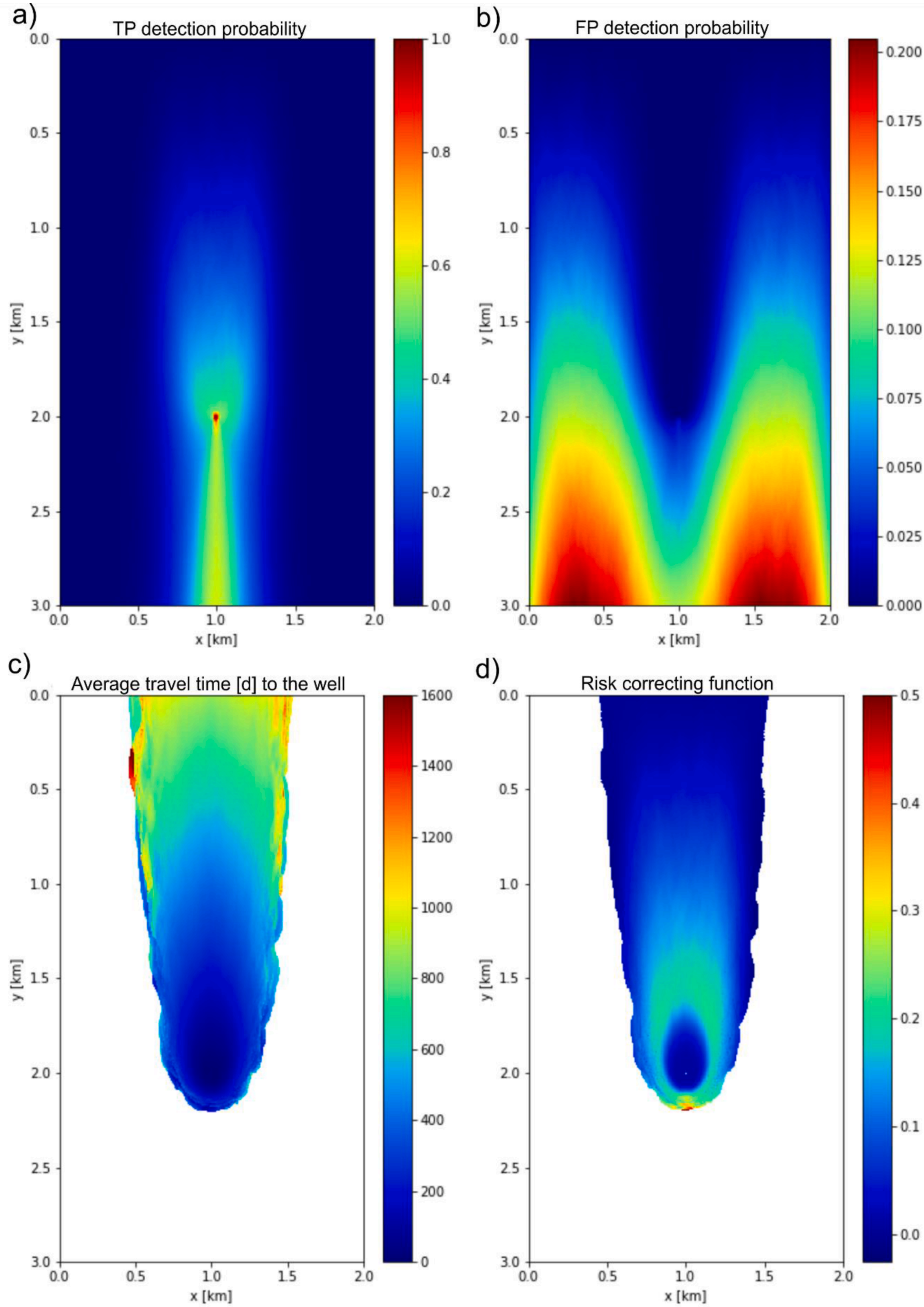

Fig. 5. a) True positive (TP) detection rate, b) false positive (FP) detection rate, c) average travel time to the pumping well, and d) the risk function; $\lambda = 50$ m, $I = 5$, $\sigma_Y^2 = 1.0$, $\alpha = 6.2$ m, $\alpha_T = 0.62$ m and $T_R = 100$ d White area. particles never reach the well.

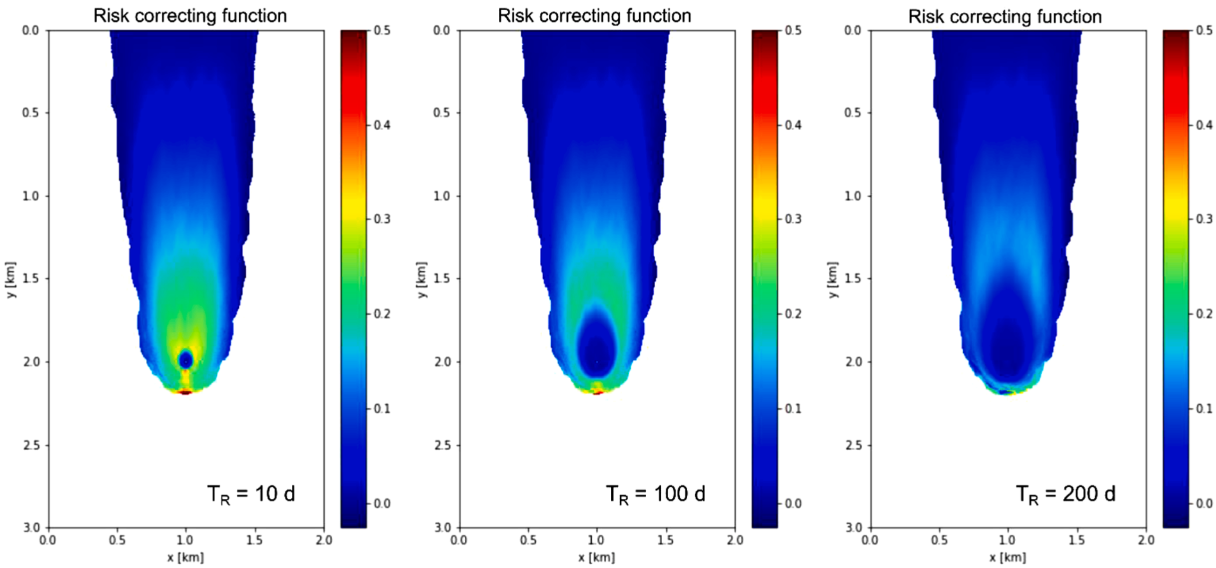

Fig. 6. The effect of travel time threshold (T_R) on f_{risk}; $\lambda = 50$ m, $I = 5$, $\sigma_Y^2 = 1.0$, $\alpha = 6.2$ m and $\alpha_T = 0.62$ m.

for uniform flow but permanent contamination source, concluded that detection probabilities continue increasing with increased dispersivities. In our study, due to the permanent source and the fact that flow and mass converge towards the pumping well, the detection rate increased even with relatively unrealistically high α_T. More dispersive conditions also result in greater f_{risk} values, while increased α^T also results in increased DFP. For the least dispersive conditions, f_{risk} peaks with 4 sentinel wells, but for all other cases and in contrast to the detection rate, f^{risk} peaks earlier with only 2 monitoring wells. This is because the marginal DTP increase of each additional well is negated by a marginal increase in false positive detections and increased travel time uncertainty (σ^T).

Figs. 7b-d show the optimal networks for varying λ, σ_Y^2 and I values. In all cases, increasing the number of monitoring wells results in increasing DTP and f_{risk} (Figs. 8b-d). For each network size, the value of these parameters appears to have only a small effect on the network spatial arrangement. As shown earlier (Fig. 4), smaller λ and σ_Y^2 result in reduced advective travel time uncertainty and greater f_{risk}. For 1 to 2 monitoring wells, DTP decreases with increasing λ, as preferential flow and transport through better connected highly permeable parts of the aquifer is more pronounced. With increasing network sizes (3 or 4 wells in our study) these preferential pathways are better intercepted, and DTP stabilizes. Increasing σ_Y^2 results in increased DTP. This is in contrast to the results of Yenigül et al. (2005) and Papapetridis and Paleologos (2011) who concluded that, for non-convergent flows, detection probabilities decrease for increased heterogeneity (σ_Y^2). The latter authors suggested that in highly heterogeneous aquifers, placing the wells closer to the known source was a necessary condition for detection to occur, suggesting that increasing σ_Y^2 potentially resulted in more dispersed plumes with concentrations below the detection limit. However under converging flow conditions this is a lesser issue, resulting in better detection of the more dispersed plumes.

The value of statistical anisotropy appears to have no effect on either DTP or f_{risk} (Fig. 8d) and only a marginal effect on the spatial distribution of the monitoring wells (Fig. 7d).

Fig. 7e shows the optimal networks with the travel time threshold T_R varied from 10 to 200 days. A low T_R value implies a much higher monitoring frequency which may increase operating costs depending on the methods used for contaminant sampling and/or measurement. As expected, increasing this threshold penalizes detections closer to the pumping well and decreases both DTP and f_{risk} (Fig. 8e), while the optimal sentinel distance from the pumping well increases to allow for earlier detection (Bode et al. 2016). When $T_R = 10$ days there is little benefit from installing more than two sentinel wells. In fact, the two wells can achieve a detection rate of 84%, and a third sentinel well only contributes an additional 1% to the estimated DTP, while its location is mostly driven by the relatively small travel time uncertainty, σ^T, resulting in marginally larger f^{risk}. Increasing T_R to 200 days reduces DTP to 24% and 70% (for 1 and 4 monitoring wells), compared to 46% and 84% for 1 and 2 monitoring wells with $T_R = 10$ days.

Discussion and practical applications

In this study a risk corrected decision analysis model is proposed to determine optimal groundwater monitoring networks for the protection of production wells. The general layout of our proposed network design stems from the "line of defense" concept proposed by Bode et al. (2016, 2018), but consisting of significantly fewer wells, due to the proposed risk correcting function and the stochastic numerical approach to the random source problem that fully considers the plume dispersion.

The focus of this study is to determine how the network detection rates are affected by aquifer heterogeneity and whether sufficient protection can be achieved from such networks. As such, certain numerical "compromises" had to be made to limit the computational burden of this study which included 216 parameter combinations, with each one requiring 15,000 flow and transport simulations. As a result, we opted to ignore seasonal variations in boundary conditions, transient transport, and multiple retarded or degrading contaminants, and represent a 3D aquifer and transport problem with a 2D numerical approximation. Even though there can be compelling cases made for all of these assumptions, it would be expected that in a practical application these may be considered in a more site-specific manner. For example, multiple contaminants based on the catchment land-uses and hydro-geochemisty can be considered, where C_{thr} values can be contaminant specific.

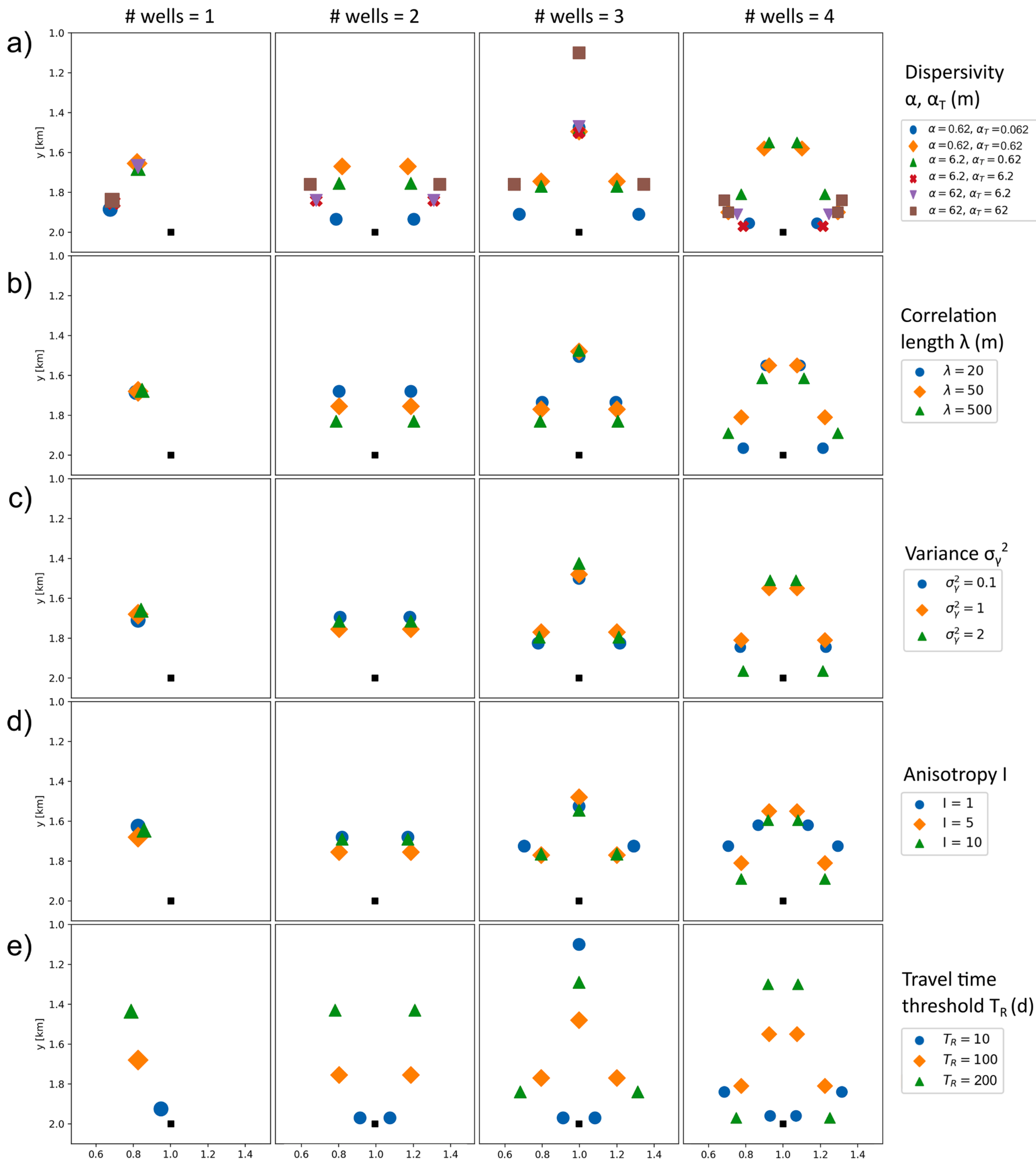

Fig. 7. Optimal monitoring networks of size 1 – 4 wells for varied aquifer parameters. The optimal networks are found by maximizing the risk correcting function (f_{risk}). a) dispersivity (in meters), b) correlation length (in meters) c) variance, d) anisotropy, e) travel time threshold (in days). DTP. TP detection rate of the network. Default parameter values are used unless otherwise specified.

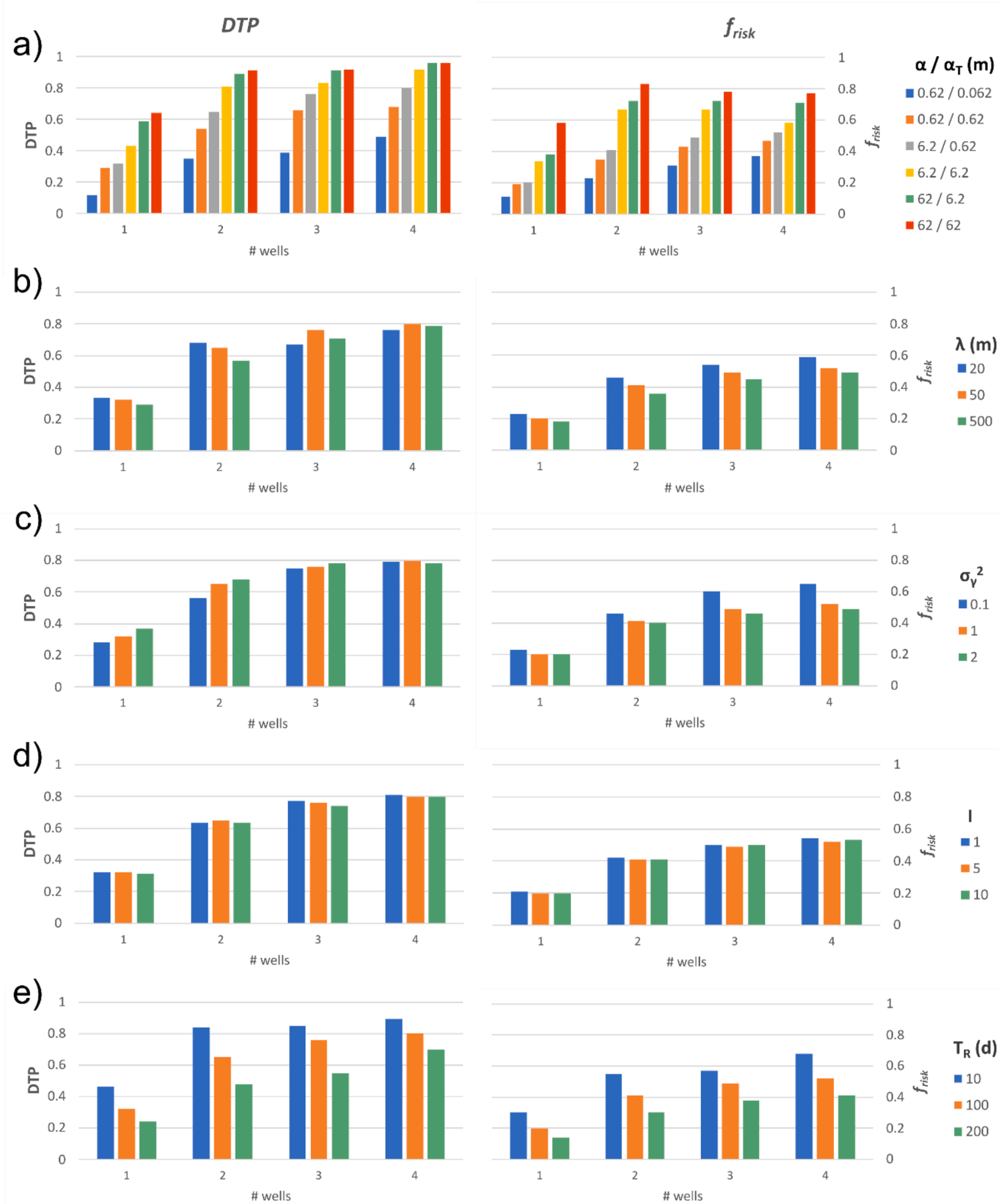

Fig. 8. TP detection probability (DTP) and risk correcting function (f_{risk}) for the optimal monitoring networks shown in the previous figure, found by maximizing f_{risk} for networks of size 1 – 4 wells and varied parameters. a) dispersivity, b) correlation length, c) variance, d) anisotropy, e) travel time threshold.

Conclusions

In this numerical study, Monte Carlo stochastic analysis is used to simulate groundwater flow and contaminant transport in a heterogeneous two-dimensional aquifer. The flow field is strongly affected by a pumping well used as a drinking water supply. Pollution originates from a steady-state source at a random location. We consider how heterogeneity and dispersion parameters affect the timely and accurate detection of contamination events of monitoring networks consisting of 1 to 4 monitoring wells. Network performance is measured as a risk correcting function considering the network's true and false positive detections, sampling frequency in terms of early detection, and the associated uncertainty. The following major conclusions can be drawn from our study:

1 Convergence of the point detection rates was not always achieved after 15,000 realizations. The true positive and true negative detection probability standard deviations were used across the field as a convergence criterion and established that 10,000 - 15,000 realizations should suffice for probabilistic solutions to stabilize. However, for highly heterogeneous and highly dispersive transport conditions, spatially distributed average values of true positive detection probabilities and advective travel time standard deviations remained nonsymmetrical even after as many as 25,000 realizations.
2 Our results indicate that in all cases of aquifer heterogeneity and dispersion, increasing the number of wells used for monitoring purposes resulted in greater detection rate of contamination events. For the base parameters of our study and from a single monitoring well it is expected that at least 32% of all contamination events that reach the water supply well would be correctly and timely identified, increasing to 80% for a network consisting of four wells. For computational reasons, our analysis was limited to a maximum of 4 monitoring wells, but detection rates of the order of 75% were achieved frequently with only 3 monitoring wells.
3 Aquifer dispersivity is the dominant parameter for the quantification of network performance. For fixed heterogeneity (λ, σ_Y^2 and I) and number of wells, detection rate increases with increased longitudinal and transverse dispersivities. Our numerical results suggest that, in contrast to previously published results for non-convergent flows and instantaneous sources, further increasing dispersion parameters does not result in detection rate reduction. Under the least dispersive conditions in our study, the detection rate is 12% and 49% for 1 and 4 monitoring wells respectively, increasing to 64% and 96% for the largest dispersivity values considered.
4 For fixed dispersion parameters, increasing spatial continuity of the Gaussian conductivity field resulted in decreased detection rate when up to two wells were considered, due to preferential flow and transport. Increasing the number of monitoring wells resulted in no obvious differences between DTP achieved for the three considered λ values, suggesting that these preferential pathways are adequately captured by the network.
5 Increasing σ_Y^2 resulted in greater detection rates for networks consisting of up to 3 wells. Once a fourth well was added to the network, σ_Y^2 did not affect the DTP. Statistical anisotropy did not appear to have a noticeable effect on the network detection rate.
6 Earlier detection for remedial action comes with a significant cost in terms of detection rate. Increasing T_R from 100 to 200 days results in 17%, 21% and 10% lower detection rates for 2, 3 and 4 monitoring wells respectively. False positive rates are also expected to increase from 1% to 4% for networks of 3 and 4 wells respectively.

Future work will expand the scope of this study to address microbial risk and non-conservative organic pollutants, under unsteady flow and transport conditions.

Declaration of Competing Interest

The authors declare that they have no known competing financial interests or personal relationships that could have appeared to influence the work reported in this paper.

Acknowledgments

The authors wish to acknowledge the two anonymous reviewers for their helpful suggestions and detailed comments that greatly improved this manuscript. This work was financed through the New Zealand Government's Strategic Science Investment Fund made available from ESR using Strategic Science Investment funding.

Supplementary materials

Supplementary material associated with this article can be found, in the online version, at doi:10.1016/j.watres.2022.118485.

References

Ayinippully Nalarajan, N., Govindarajan, S.K., Nambi, I.M., 2021. Aquifer heterogeneity on well capture zone and solute transport: numerical investigations with spatial moment analysis. Int. J. Environ. Sci. Technol. https://doi.org/10.1007/s13762-021-03573-y.
Bear, J., 1979. Hydraulics of Groundwater. McGraw-Hill, New York, p. 569.
Bedekar, V., Morway, E.D., Langevin, C.D., Tonkin, M.J., 2016. MT3D-USGS Version 1: A U.S. Geological Survey Release of MT3DMS Updated With New and Expanded Transport Capabilities For Use With MODFLOW. Techniques and Methods, Reston, VA.
Bierkens, M.F.P., 2006. Designing a monitoring network for detecting groundwater pollution with stochastic simulation and a cost model. Stochastic Environ. Res. Risk Assess. 20 (5), 335–351 doi: 10.1007/s00477-005-0025-2.
Bode, F., Ferré, T., Zigelli, N., Emmert, M., Nowak, W., 2018. Reconnecting stochastic methods with hydrogeological applications: a utilitarian uncertainty analysis and risk assessment approach for the design of optimal monitoring networks. Water Resour. Res. 54 (3), 2270–2287 doi: https://doi.org/10.1002/2017WR020919.
Bode, F., Nowak, W., Loschko, M., 2016. Optimization for early-warning monitoring networks in well catchments should be multi-objective, risk-prioritized and robust against uncertainty. Transp. Porous Media 114 (2), 261–281 doi: 10.1007/s11242-015-0586-6.
Bolster, D., Barahona, M., Dentz, M., Fernandez-Garcia, D., Sanchez-Vila, X., Trinchero, P., Valhondo, C., Tartakovsky, D.M., 2009. Probabilistic risk analysis of groundwater remediation strategies. Water Resour. Res. 45 (6) doi: https://doi.org/10.1029/2008WR007551.
Bortone, I., Chianese, S., Erto, A., Di Nardo, A., De Crescenzo, C., Karatza, D., Santonastaso, G.F., Musmarra, D., 2019. An optimized configuration of adsorptive wells for the remediation of an aquifer contaminated by multiple aromatic hydrocarbon pollutants. Sci. Total Environ. 696, 133731 doi: https://doi.org/10.1016/j.scitotenv.2019.133731.
Burbery, L., Sarris, T., Mellis, R., Abraham, P., Sutton, R., Finnemore, M., Close, M., 2020. Woodchip denitrification wall technology trialled in a shallow alluvial gravel aquifer. Ecol. Eng. 157, 105996 doi: https://doi.org/10.1016/j.ecoleng.2020.105996.
Burbery, L.F., Moore, C.R., Jones, M.A., Abraham, P.M., Humphries, B.L., Close, M.E., Ventra, D., Clarke, L.E., 2018. Study of connectivity of open framework gravel facies in the Canterbury Plains aquifer using smoke as a tracer. Geology and Geomorphology of Alluvial and Fluvial Fans: Terrestrial and Planetary Perspectives, 0. Geological Society of London.
Cole, B.E., Silliman, S.E., 1997. Capture Zones for Passive Wells in Heterogeneous Unconfined Aquifers. Groundwater 35 (1), 92–98 doi: https://doi.org/10.1111/j.1745-6584.1997.tb00064.x.
Da'ana, D.A., Zouari, N., Ashfaq, M.Y., Abu-Dieyeh, M., Khraisheh, M., Hijji, Y.M., Al-Ghouti, M.A., 2021. Removal of toxic elements and microbial contaminants from groundwater using low-cost treatment options. Curr. Pollution Reports 7 (3), 300–324 doi: 10.1007/s40726-021-00187-3.
de Barros, F.P.J., Bellin, A., Cvetkovic, V., Dagan, G., Fiori, A., 2016. Aquifer heterogeneity controls on adverse human health effects and the concept of the hazard attenuation factor. Water Resour. Res. 52 (8), 5911–5922 doi: https://doi.org/10.1002/2016WR018933.
Deutsch, C.V., Journel, A.G., 1997. GSLIB : Geostatistical Software Library and User's Guide. Oxford University Press, New York, 2nd ed.
Donaldson, I.G., Campbell, D.G., 1977. Groundwaters of the Hutt Valley – Port Nicholson alluvial basin. DSIR information series No 124, 78.
Elkhoury, J.E., Brodsky, E.E., Agnew, D.C., 2006. Seismic waves increase permeability. Nature 441 (7097), 1135–1138 doi: 10.1038/nature04798.
Fang, Y., Qian, B., Yang, Y., Song, Y., Yang, Z., Li, H., 2022. Purification of high-arsenic groundwater by magnetic bimetallic MOFs coupled with PMS: balance of catalysis and adsorption and promotion mechanism of PMS. Chem. Eng. J. 432, 134417 doi: https://doi.org/10.1016/j.cej.2021.134417.

Fiori, A., Dagan, G., Jankovic, I., Zarlenga, A., 2013. The plume spreading in the MADE transport experiment: could it be predicted by stochastic models? Water Resour. Res. 49 (5), 2497–2507 doi: https://doi.org/10.1002/wrcr.20128.
Frind, E.O., Molson, J.W., 2018. Issues and options in the delineation of well capture zones under uncertainty. Groundwater 56 (3), 366–376 doi: https://doi.org/10.1111/gwat.12644.
Gelhar, L.W., 1986. Stochastic subsurface hydrology from theory to applications. Water Resour. Res. 22 (9S), 135S-145S. doi: 10.1029/WR022i09Sp0135S.
Gibert, O., Abenza, M., Reig, M., Vecino, X., Sánchez, D., Arnaldos, M., Cortina, J.L., 2022. Removal of nitrate from groundwater by nano-scale zero-valent iron injection pulses in continuous-flow packed soil columns. Sci. Total Environ. 810, 152300 doi: https://doi.org/10.1016/j.scitotenv.2021.152300.
Gómez-Hernández, J.J., Butler, J.J., Fiori, A., Bolster, D., Cvetkovic, V., Dagan, G., Hyndman, D., 2017. Introduction to special section on Modeling highly heterogeneous aquifers: lessons learned in the last 30 years from the MADE experiments and others. Water Resour. Res. 53 (4), 2581–2584 doi: https://doi.org/10.1002/2017WR020774.
Gyopari, M., 2014. Lower Hutt aquifer model revision (HAM3): sustainable management of the Waiwhetu Aquifer. Greater Wellington Regional Council Report 224p.
Hudak, P.F., 2001. Effective contaminant detection networks in uncertain groundwater flow fields. Waste Manage. (Oxford) 21 (4), 309–312 doi: https://doi.org/10.1016/S0956-053X(00)00079-9.
Hudak, P.F., 2002. Efficiency comparison of graphical approaches for designing contaminant detection networks in groundwater. Water Resour. Res. 38 (12), 18-1-18-5. doi: 10.1029/2001wr001152.
Hudak, P.F., 2005. Sensitivity of groundwater monitoring networks to contaminant source width for various seepage velocities. Water Resour. Res. 41 (8), 1–4 doi: 10.1029/2005WR003968.
Ishii, E., Watanabe, Y., Agusa, T., Hosono, T., Nakata, H., 2021. Acesulfame as a suitable sewer tracer on groundwater pollution: a case study before and after the 2016 Mw 7.0 Kumamoto earthquakes. Sci. Total Environ. 754, 142409 doi: https://doi.org/10.1016/j.scitotenv.2020.142409.
Kang, G.-C., Tobita, T., Iai, S., 2013. Damage to sewerage systems during the 2004 Earthquake in Niigata-ken Chuetsu, Japan. Eng. Geol. 164, 230–242 doi: https://doi.org/10.1016/j.enggeo.2013.07.011.
Kobayashi, J., Kuroda, K., Miyamoto, C., Uchiyama, Y., Sankoda, K., Nakajima, D., 2021. Evaluating sewer exfiltration in groundwater by pharmaceutical tracers after the 2016 Kumamoto earthquakes, Japan. J. Hazard. Mater. 411, 125183 doi: https://doi.org/10.1016/j.jhazmat.2021.125183.
Lahkim, M.B., Garcia, L.A., 1999. Stochastic Modeling of Exposure and Risk in a Contaminated Heterogeneous Aquifer. 1: monte Carlo Uncertainty Analysis. Environ. Eng. Sci. 16 (5), 315–328 doi: 10.1089/ees.1999.16.315.
Liu, C.-P., Wang, C.-H., Hwang, L.-S., 2010. Temporal variation of seepage water chemistry before and after the Hengchun Ms 7.2 earthquake in south Taiwan. Geoderma 155 (1), 107–114 doi: https://doi.org/10.1016/j.geoderma.2009.12.001.
Mahjouri, N., Shamsoddinpour, M., 2016. Developing a methodology for early leakage detection in landfills: application of the fuzzy transformation technique and probabilistic artificial neural networks. Environ. Earth Sci. 75 (12) doi: 10.1007/s12665-016-5757-4.
Meyer, P.D., Valocchi, A.J., Eheart, J.W., 1994. Monitoring network design to provide initial detection of groundwater contamination. Water Resour. Res. 30 (9), 2647–2659 doi: 10.1029/94wr00872.
Moreira, N.A., Bondelind, M., 2016. Safe drinking water and waterborne outbreaks. J. Water Health 15 (1), 83–96 doi: 10.2166/wh.2016.103.
Nakagawa, K., Shimada, J., Yu, Z.-Q., Ide, K., Berndtsson, R., 2021. Effects of the Japanese 2016 Kumamoto Earthquake on Nitrate Content in Groundwater Supply. Minerals 11 (1), 43.
Niswonger, R.G., Panday, S., Ibaraki, M., 2011. A Newton formulation for MODFLOW-2005. U.S. Geol. Surv. Techn. Methods, 6–A37:44pp.
Nowak, W., Bode, F., Loschko, M., 2015. A multi-objective optimization concept for risk-based early-warning monitoring networks in well catchments. Procedia Environ. Sci. 25, 191–198 doi: https://doi.org/10.1016/j.proenv.2015.04.026.
Onyango, L.A., Quinn, C., Tng, K.H., Wood, J.G., Leslie, G., 2015. A study of failure events in drinking water systems as a basis for comparison and evaluation of the efficacy of potable reuse schemes. Environ. Health Insights 9s3. EHI.S31749. doi: 10.4137/ehi.S31749.
Pagano, M., Gauvreau, K., 2018. Principles of Biostatistics. CRC Press.
Paleologos, E.K., Sarris, T.S., 2011. Stochastic analysis of flux and head moments in a heterogeneous aquifer system. Stochastic Environ. Res. Risk Assess. 25 (6), 747–759 doi: 10.1007/s00477-011-0459-7.
Paleologos, E.K., Sarris, T.S., Desbarats, A., 2000. Numerical estimation of effective hydraulic conductivity in leaky heterogeneous aquitards. Theory, modeling, and Field Investigation in hydrogeology: a Special Volume in Honor of Shlomo P. Neumans 60th Birthday. Geological Society of America edited by Shlomo P. Neuman, Dongxiao Zhang and C. Larry Winter, 119-127.
Papapetridis, K., Paleologos, E.K., 2011. Contaminant detection probability in heterogeneous aquifers and corrected risk analysis for remedial response delay. Water Resour. Res. 47 (10) doi: 10.1029/2011wr010652.
Papapetridis, K., Paleologos, E.K., 2012. Sampling Frequency of Groundwater Monitoring and Remediation Delay at Contaminated Sites. Water Resour. Manage. 26 (9), 2673–2688 doi: 10.1007/s11269-012-0039-8.
Pollock, D.W. 1994. "User's Guide for MODPATH/MODPATH-PLOT, Version 3: a Particle Tracking Post-processing Package for MODFLOW, the US: geological Survey Finite-difference Ground-water Flow Model".
Renou, S., Givaudan, J.G., Poulain, S., Dirassouyan, F., Moulin, P., 2008. Landfill leachate treatment: review and opportunity. J. Hazard. Mater. 150 (3), 468–493 doi: 10.1016/j.jhazmat.2007.09.077.
Ruppert, M., V. Bertsch, W. Fichtner, and Ieee. 2015. "Optimal load shedding in distributed networks with sigmoid cost functions". 2015 International Symposium on Smart Electric Distribution Systems and Technologies (EDST), Vienna, AUSTRIA, Sep 07-11.
Salamon, P., Fernàndez-Garcia, D., Gómez-Hernández, J.J., 2006. Modeling mass transfer processes using random walk particle tracking. Water Resour. Res. 42 (11), 1–14 doi: 10.1029/2006WR004927.
Sarikaya, H.Z., and I. Koyuncu. 1999. "Evaluation of the Effects of Kocaeli earthquake On Water and Wastewater Systems", International Conference on the Kocaeli Earthquake, Istanbul Tech Univ, Istanbul, Turkey, Dec 02-05.
Sarris, T.S., Burbery, L.F., 2018. Stochastic multi-objective performance optimization of an in-stream woodchip denitrifying bioreactor. Ecol. Eng. 124, 38–50 doi: https://doi.org/10.1016/j.ecoleng.2018.09.006.
Sarris, T.S., Close, M., Abraham, P., 2018. Using solute and heat tracers for aquifer characterization in a strongly heterogeneous alluvial aquifer. J. Hydrol. 558, 55–71 doi: 10.1016/j.jhydrol.2018.01.032.
Sarris, T.S., Close, M.E., Moore, C., 2019a. Uncertainty assessment of nitrate reduction in heterogeneous aquifers under uncertain redox conditions. Stochastic Environ. Res. Risk Assess. 33 (8–9), 1609–1627 doi: 10.1007/s00477-019-01715-w.
Sarris, T.S., Paleologos, E.K., 2004. Numerical investigation of the anisotropic hydraulic conductivity behavior in heterogeneous porous media. Stochastic Environ. Res. Risk Assess. 18 (3), 188–197 doi: 10.1007/s00477-003-0171-3.
Sarris, T.S., Scott, D.M., Close, M.E., 2021. Parallel simulation in subsurface hydrology: evaluating the performance of modelling computers. Groundwater 59, 109–116 doi: 10.1111/gwat.13024.
Sarris, T.S., Scott, D.M., Close, M.E., Humphries, B., Moore, C., Burbery, L.F., Rajanayaka, C., Barkle, G., Hadfield, J., 2019b. The effects of denitrification parameterization and potential benefits of spatially targeted regulation for the reduction of N-discharges from agriculture. J. Environ. Manage. 247, 299–312 doi: 10.1016/j.jenvman.2019.06.074.
Sreekanth, J., Lau, H., Pagendam, D.E., 2017. Design of optimal groundwater monitoring well network using stochastic modeling and reduced-rank spatial prediction. Water Resour. Res. 53 (8), 6821–6840 doi: https://doi.org/10.1002/2017WR020385.
Storck, P., Eheart, J.W., Valocchi, A.J., 1997. A method for the optimal location of monitoring wells for detection of groundwater contamination in three-dimensional heterogeneous aquifers. Water Resour. Res. 33 (9), 2081–2088 doi: 10.1029/97WR01704.
USEPA, 1987. Guidelines For Delineation of Wellhead Protection areas: United States Environmental Protection Agency. Office of Ground Water Protection.
Wang, C.-Y., Liao, X., Wang, L.-P., Wang, C.-H., Manga, M., 2016. Large earthquakes create vertical permeability by breaching aquitards. Water Resour. Res. 52 (8), 5923–5937 doi: https://doi.org/10.1002/2016WR018893.
Wang, C.-y., Wang, C.-H., Manga, M., 2004. Coseismic release of water from mountains: evidence from the 1999 (Mw = 7.5) Chi-Chi, Taiwan, earthquake. Geology 32 (9), 769–772 doi: 10.1130/g20753.1.
Wang, Y., Wang, X., Chau, H.W., Si, B., Yao, N., Li, Y., 2018. Water movement and finger flow characterization in homogeneous water-repellent soils. Vadose Zone J. 17 (1), 1–12 doi: 10.2136/vzj2018.01.0021.
Winter, C.L., Tartakovsky, D.M., 2008. A reduced complexity model for probabilistic risk assessment of groundwater contamination. Water Resour. Res. 44 (6) doi: https://doi.org/10.1029/2007WR006599.
Yenigül, N.B., Elfeki, A.M.M., Gehrels, J.C., van den Akker, C., Hensbergen, A.T., Dekking, F.M., 2005. Reliability assessment of groundwater monitoring networks at landfill sites. J. Hydrol. 308 (1), 1–17 doi: https://doi.org/10.1016/j.jhydrol.2004.10.017.
Yenigül, N.B., Elfeki, A.M.M., van den Akker, C., Dekking, F.M., 2013. Optimizing groundwater monitoring systems for landfills with random leaks under heterogeneous subsurface conditions. Hydrol. J. 21 (8), 1761–1772 doi: 10.1007/s10040-013-1013-0.
Yerushalmy, J., 1947. Statistical Problems in Assessing Methods of Medical Diagnosis, with Special Reference to X-Ray Techniques. Public Health Rep. (1896-1970) 62 (40):1432-1449. doi: 10.2307/4586294.
Zech, A., Attinger, S., Cvetkovic, V., Dagan, G., Dietrich, P., Fiori, A., Rubin, Y., Teutsch, G., 2015. Is unique scaling of aquifer macrodispersivity supported by field data? Water Resour. Res. 51 (9), 7662–7679 doi: 10.1002/2015WR017220.
Zhang, H., Shi, Z., Wang, G., Sun, X., Yan, R., Liu, C., 2019. Large Earthquake Reshapes the Groundwater Flow System: insight From the Water-Level Response to Earth Tides and Atmospheric Pressure in a Deep Well. Water Resour. Res. 55 (5), 4207–4219 doi: https://doi.org/10.1029/2018WR024608.
Zheng, C., Wang, P.P., 1999. MT3DMS: A Modular Three-Dimensional Multispecies Transport Model For Simulation of Advection, Dispersion and Chemical Reactions of Contaminants in Groundwater Systems; Documentation and User's Guide. US Army Corps of Engineers-Engineer Research and Development Center, Vicksburg, MS.
Zhu, L., Gong, H., Dai, Z., Guo, G., Teatini, P., 2017. Modeling 3-D permeability distribution in alluvial fans using facies architecture and geophysical acquisitions. Hydrol. Earth Syst. Sci 21 (2), 721–733 doi: 10.5194/hess-21-721-2017.